

Waves, Turbulence and Mixing Parameterizations

E. A. D’Asaro

Applied Physics Laboratory, University of Washington, Seattle, WA

R. C. Lien

Applied Physics Laboratory and School of Oceanography, University of Washington, Seattle, WA

Abstract. Recent measurements of Lagrangian frequency spectra in both the open ocean and Knight Inlet have led to a new way to separate internal waves and turbulence. Internal waves are found to have Lagrangian frequencies greater than N , while turbulence has Lagrangian frequencies less than N . This also leads to a new understanding of how mixing changes with increasing energy, i.e., decreasing Richardson number. At high Richardson number, mixing is controlled by interactions between internal wave modes. At Richardson number of order 1, mixing is controlled by instabilities of the wave modes. A “Wave-Turbulence” (W-T) transition separates these two regimes. As viewed in terms of vertical wavenumber spectra, the W-T transition occurs when the internal wave bandwidth becomes small thus suppressing wave-wave interactions. As viewed in terms of Lagrangian (intrinsic) frequency spectra, the transition occurs when the inertial subrange of turbulence, confined to frequencies greater than N , reaches the level of the internal waves, confined to frequencies less than N . Present parameterizations of oceanic turbulence predict that these two singularities in the spectra occur at the same energy level. At internal wave energies below the W-T transition, dissipation rate depends on the internal wave energy squared; above the transition the dependence is linear. The finite depth of the water is crucial to the transition; the transition occurs at a lower shear and dissipation rate in shallower water. Traditional turbulence closure models, i.e., Mellor-Yamada and its relatives, ignore internal waves and will be accurate only at energies above the W-T transition.

Introduction

Two very different classes of models have been used to understand turbulence and mixing in stratified geophysical flows. One approach attempts to extrapolate the physics of unstratified turbulence into the stratified regime. Such “Stratified Turbulence” models (*Mellor and Yamada* [1982], *Luyten et al.* [1996]) work well if the stratification is not too strong and the flow remains highly turbulent, but fail if the stratification is too strong [*Simp-*

son et al., 1996]. A second approach attempts to extrapolate the physics of waves into a partially turbulent regime. Such “Wave-Wave Interaction” models [*Müller et al.*, 1986] work well in the weakly turbulent ocean thermocline (*Gregg* [1989]; *Polzin et al.* [1995]) and have not been well tested in other regimes. The two classes of models are fundamentally different in physical assumptions and mathematical form and will yield very different results if applied to the same flow.

The two different classes of models are designed to operate in different Richardson number regimes. Wave-wave interaction models assume that the flow can be expressed as the sum of interacting internal waves, each of which is a solution to the inviscid linear internal wave equations. Energy transfer and fluxes occur through the interactions of these waves. This approach is appropriate at high Richardson number, where the waves are stable and interact only weakly. Stratified turbulence models generally parameterize fluxes by assuming a local turbulent eddy viscosity, or similar closure, whose strength depends on the local length and time scales of the flow. This approach is appropriate at low Richardson number where the flow is mostly turbulent and waves play only a minor role [Henyey, 1989]. A transition from the high Richardson number wave physics to the low Richardson number turbulent physics should occur at some intermediate Richardson number. We will call this the *Wave to Stratified Turbulence Transition* or W-T transition.

We will study the W-T transition from an oceanographic viewpoint, considering how the physics of a broadband, high Richardson number, internal wave field, such as that in the open ocean thermocline, changes as its energy increases. The analysis is based on the observed shapes of oceanic spectra and existing parameterizations of dissipation rate. We first consider the Lagrangian frequency spectra of velocity, a recently measured quantity, first briefly describing the recent observations. We then consider the Eulerian wavenumber spectra of shear, a quantity that is well measured and modeled in the oceanic thermocline. Neither spectra can maintain its low energy form at high energy, implying that a transition must occur. We then quantify the transition and find that both spectra lose their low energy form at the energy level at which the large-scale Richardson number drops below 1.

Lagrangian Frequency Spectrum

Lien *et al.* [1998] and D'Asaro and Lien [1999] describe frequency spectra ($\Phi_u(\omega)$, $\Phi_v(\omega)$, $\Phi_w(\omega)$)

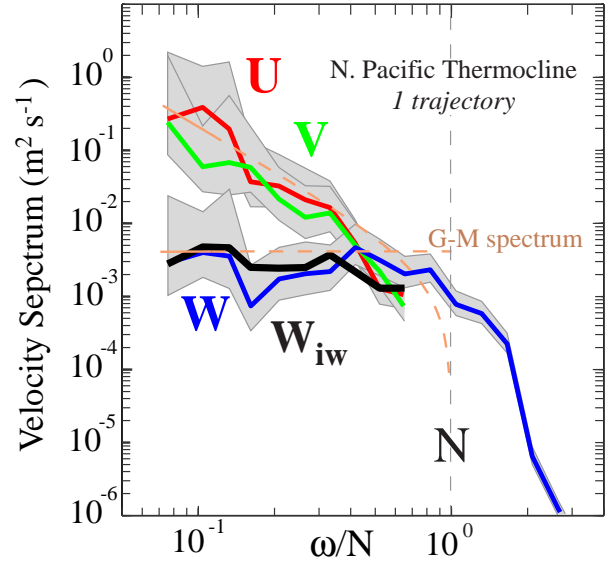


Figure 1. Normalized east (red), north (green) and vertical (blue) velocity spectra from the North Pacific thermocline. Shading represents the 95% confidence interval. Black line (W_{iw}) is the vertical velocity spectrum computed from (1). Orange dashed lines are the GM spectrum. (A color version of this figure is shown in the special section of these proceedings).

[m^2s^{-1}] of velocity (u, v, w) as a function of Lagrangian frequency, ω [s^{-1}], as observed by neutrally buoyant floats in regions of both strong and weak turbulence. Their key diagnostic is the internal wave consistency relationship (Fofonoff [1969], Calman [1978])

$$\frac{\Phi_w^{iw}}{\Phi_H^{iw}} = \frac{\omega^2(\omega^2 - f^2)}{(N^2 - \omega^2)(\omega^2 + f^2)} \quad (1)$$

where $\Phi_H^{iw} = \Phi_u^{iw} + \Phi_v^{iw}$.

Figure 1 shows spectra of horizontal and vertical velocity from an open ocean site. The spectra lie very close to the Garrett-Munk spectrum (orange dashed line) for frequencies below N . The vertical velocity spectrum falls rapidly above N . The black line marked W_{iw} shows the vertical velocity spectrum computed from (1) assuming that the horizontal velocity spectrum is entirely due to internal waves. If (1) is true, W_{iw} should equal W .

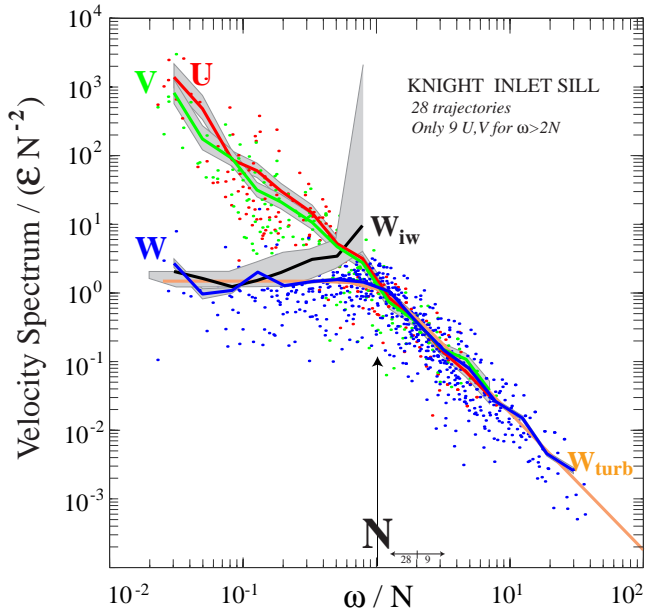


Figure 2. Normalized east (red), north (green), and vertical (blue) velocity spectra from the Knight Inlet sill. Dots are individual spectral estimates corrected for instrumental response; lines are average of these; shading represents the 95% confidence interval. Black line (W_{iw}) is the vertical velocity spectrum computed from (1) assuming that horizontal spectra are entirely due to internal waves. (A color version of this figure is shown in the special section of these proceedings).

W_{iw} lies within the error bars for W up to about $0.4 N$. Velocity fluctuations at this open ocean site are therefore dominated by internal waves, as expected. Analyses like this are the major reason why we think that internal waves dominate high frequency fluctuations in the open ocean.

Figure 2 shows 28 spectra taken near the sill of Knight Inlet, a region of strong turbulence and mixing. The motions with frequencies below N have the properties expected of internal waves: they are anisotropic, approximately as specified by (1), and they have approximately the Garrett-Munk spectral shape characteristic of internal waves. This is truly remarkable; The sill of Knight Inlet is not where you would expect to find a Garrett-Munk spectrum! The motions with frequencies above N have the properties expected of homogeneous turbulence: their spectra

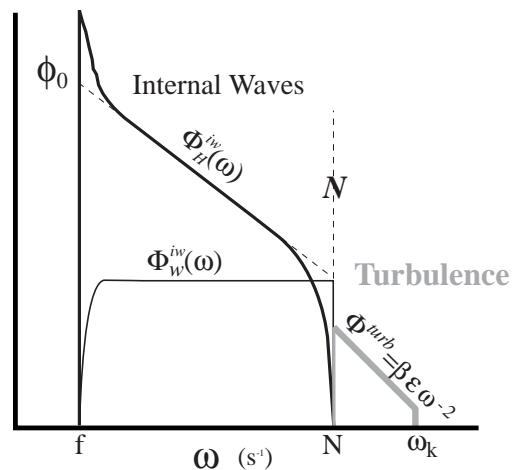


Figure 3. Model Lagrangian frequency spectra of vertical (w) and horizontal (H) velocity. The model consists of separate internal wave and turbulent components.

are isotropic, and they have the -2 spectral shape characteristic of homogeneous turbulence. Based on these results *D'Asaro and Lien* [1999] hypothesize that the buoyancy frequency, measured in Lagrangian coordinates, separates waves and turbulence.

Based on these observations, we propose the Lagrangian frequency spectrum shown in Figure 3. It is the sum of internal wave and turbulent components. We model the internal wave horizontal velocity spectrum following GM76 [*Gregg and Kunze*, 1991], a traditional combination of *Garrett and Munk* [1975] and *Cairns and Willaims* [1976],

$$\Phi_H^{iw}(\omega) = \phi_0 \frac{f^2}{\omega(\omega^2 - f^2)^{1/2}} B\left(\frac{\omega}{N}\right) \quad (2)$$

where ϕ_0 is a constant which sets the internal wave energy, and B describes the shape of the spectrum near N . For $N \gg \omega \gg f$, Φ_H^{iw} has a -2 slope and Φ_w^{iw} is white. Observed Φ_w sometimes show peaks near $\omega = N$. We will ignore these and choose

$$B(\omega) = (N^2 - \omega^2)/N^2 \quad (3)$$

so as to make Φ_w^{iw} white near N . Accordingly, Φ_H^{iw} falls below Φ_w^{iw} between $N/2^{1/2}$ and N .

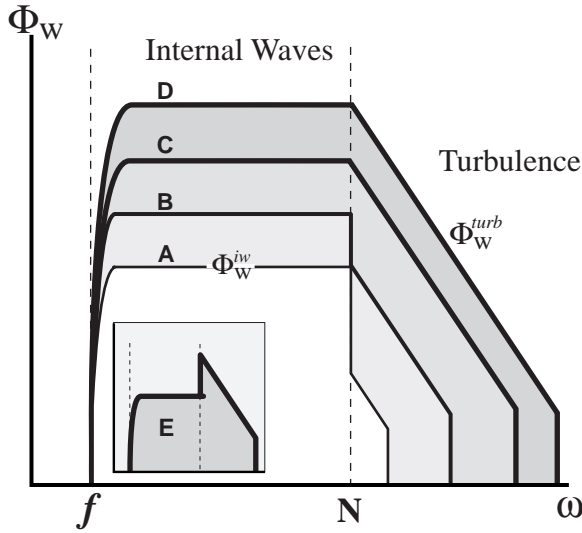


Figure 4. Evolution of Lagrangian frequency spectrum of vertical velocity with increasing energy. Spectra A and B are below the W-T transition energy. Spectrum C is just at the transition energy. Spectra D and E are two possible spectra above the transition energy. Spectrum E is not observed to occur.

Motions with Lagrangian frequencies above N are due to turbulence. We assume isotropic turbulence, $\Phi_H^{turb}/2 = \Phi_w^{turb} \equiv \Phi^{turb}$. For $\omega > N$, the spectrum is described by an inertial subrange (Corrsin [1963], Lien *et al.* [1998])

$$\Phi^{turb}(\omega) = \frac{\beta\varepsilon}{\omega^2}, \quad (\omega > N) \quad (4)$$

with a Kolmogorov constant β , which has a value between 1 and 2 [Lien *et al.*, 1998]. We use $\beta = 1.8$. The inertial subrange form should be correct only for frequencies much larger than a “Large-Eddy” frequency, here taken to be N , and much less than a Kolmogorov frequency $\omega_k = (\varepsilon/\nu)^{1/2}$. D’Asaro and Lien [1999] give analytical forms for the exact spectral shape of the spectrum near N . We assume no turbulent energy for frequencies below N

$$\Phi^{turb}(\omega) = 0 \quad (\omega < N) \quad (5)$$

although this must certainly be an approximation.

Figure 4 shows the evolution of the model $\Phi_w(\omega)$ as a function of internal wave energy. For typi-

cal oceanic, i.e., Garrett-Munk or GM, energy levels, (spectrum A), the internal wave spectrum has far more energy than the turbulence spectrum. This results in the sharp drop in the spectrum near N . This drop is particularly sharp when observed from neutrally buoyant floats (Cairns [1975], D’Asaro and Lien [1999], Kunze *et al.* [1990]), i.e. for Lagrangian spectra. However, since the value of ε increases quadratically with wave energy (Gregg [1989]; Polzin *et al.* [1995]) the ratio $\Phi_w^{turb}(N)/\Phi_w^{iw}(N)$ will be proportional to $\Phi_w^{iw}(N)$. At low energies (spectrum A), the ratio will be small. As the internal wave energy increases (spectrum B), the ratio will increase until it reaches 1 (spectrum C). At this energy, which will turn out to mark the W-T transition, the drop in spectral level at N has disappeared.

If the energy is increased above the W-T transition level there are two possibilities: Φ_w^{turb} could continue to increase quadratically, as shown in spectrum E (Fig.4, insert), leading to a sharp increase in spectral level at N , or it could remain at the same level as Φ_w^{iw} as shown in spectrum D. D’Asaro and Lien [1999] (Fig.2) find no spectra which look like E, but many spectra which look like D. We therefore assume that only spectrum D occurs. D’Asaro and Lien [1999] assume this and using the analytical spectral shapes near N , find

$$\varepsilon = 1.2 \beta^{-1} \Phi_w^{iw} N^2 = 0.6 \beta^{-1} \sigma_w^2 N \quad (6)$$

where σ_w^2 is the total vertical velocity variance. This relationship, valid at or above the W-T transition, shows a linear relationship between energy and dissipation. Thus the W-T transition marks a change from a quadratic to a linear relationship between energy and turbulent dissipation rate.

Eulerian Wavenumber Spectrum

Spectral Form

The vertical wavenumber spectrum, $\Phi_{SS}(m)$, of horizontal shear, S , in the ocean thermocline has been measured by many investigators using vertical profilers [Gregg, 1991]. Measurements have

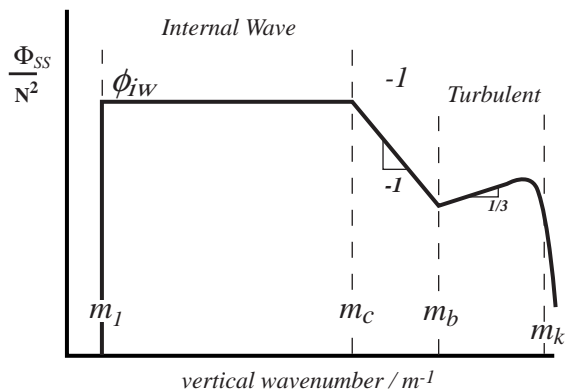


Figure 5. Model spectra of vertical wavenumber spectrum of shear.

been mostly at near-GM energy levels. The basic form, first proposed by *Garrett et al.* [1981], is shown in Figure 5. There are three wavenumber bands: a low wavenumber “Internal Wave” band, a high wavenumber “Turbulence” band and an intermediate “-1” band named for its spectral slope. We will extrapolate this form to energies much higher than GM and show how it eventually fails.

The low wavenumber band is believed to be dominated by internal waves [*Müller et al.*, 1978]. We assume a white normalized shear spectrum, $\Phi_{SS}(m)/N^2$ with a level ϕ_{iw} , consistent with numerous observations (*Gregg et al.* [1993]; *Polzin et al.* [1995]). The lower end of the internal wave band is set by the WKB-stretched wavelength of the gravest internal wave mode, m_1 . For the open ocean, this is set by the thermocline depth; we assume the GM76 value $m_1 = 2\pi/b$ [m^{-1}] with $b = 1300 m$. For the continental shelf, this is set by the water depth; we will use $b = 100 m$. In the Garrett-Munk spectrum the shear spectral slope changes from white to +2 below vertical mode number j^* . GM76 uses $j^* = 3$. *Levine et al.* [1997] show evidence that j^* is large for low energy internal wave fields. Measurements under a storm [*D’Asaro*, 1985] and on the continental shelf (M. Levine, personal communication 1999) suggest that j^* is small for high energy internal wave fields. The data therefore suggest that at energies sub-

stantially above GM, j^* probably falls below 1 and the spectrum is white down to the lowest mode. We therefore ignore the j^* factor in GM76 and retain a white shear spectrum all the way to the lowest mode.

The upper end of the internal wave band is set by a critical wavenumber, m_c (*Munk* [1981], *Sherman and Pinkel* [1991]) at which the Richardson number becomes small. More formally, the value of m_c is set so that the Froude function

$$Fr(m) = \int_{m_1}^m \frac{\Phi_{SS}(m)}{N^2} dm \quad (7)$$

equals a critical value, i.e. $Fr(m_c) = Fr_c$. *Polzin et al.* [1995] uses $Fr_c = 0.7$. This yields

$$\phi_{iw}(m_c - m_1) = Fr_c. \quad (8)$$

Previous investigators have ignored the finite depth of the ocean, assuming $m_1 \ll m_c$, and thus written (8) with $m_1 = 0$. We will show that the W-T transition occurs when m_1 and m_c become comparable. Computationally, however, there is little advantage to including m_1 in (7) and (8), since it only becomes important when the model fails. Furthermore, including it leads to violation of Ozmidov scaling at high energies which seems unphysical. We therefore set $m_1 = 0$ and extrapolate the model to high energy to find how this, and other assumptions, fail.

At wavenumbers above m_c the spectral slope changes to -1. At wavenumbers above $m_b = (N^3/\varepsilon)^{1/2}$, corresponding to the inverse Ozmidov and overturning [*Dillon*, 1982] length scales, the spectrum assumes the form of the turbulent “-5/3” inertial subrange

$$\Phi_{SS}^{turb} = m^2 \Phi_u^{turb} = \alpha_E \varepsilon^{2/3} m^{1/3} \quad (9)$$

out to the Kolomogorov (viscous) wavenumber $m_k = (\varepsilon/\nu^3)^{1/4}$. The Kolmogorov constant is $\alpha_E = 0.5$, to an accuracy of 10% [*Sreenivasan*, 1995]. The dynamical nature of the “-1” range, intermediate between the internal waves and turbulence, remains elusive despite numerous observations of its existence in the ocean and atmosphere [*Gregg et al.*, 1993].

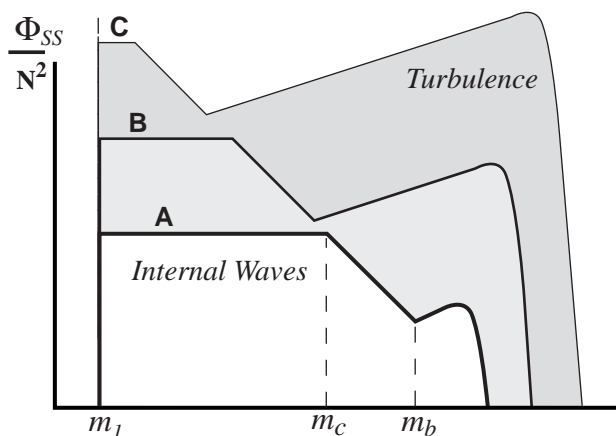


Figure 6. Evolution of model vertical wavenumber spectra of shear with increasing energy. Spectrum A is close to GM energy. With increasing energy the bandwidth of the internal waves shrinks and the bandwidth of turbulence increases. Spectrum D is close to the Wave-Turbulence transition.

Figure 6 shows the evolution of the vertical wavenumber spectrum with increasing energy as in Fig.4. At the GM level (spectrum A), the internal wave bandwidth, $m_c - m_1$ is large, since $m_c \gg m_1$ and the turbulence bandwidth is small, since m_k is not very much bigger than m_b . With increasing energy (Spectra B-C), the internal wave bandwidth shrinks as m_c approaches m_1 and the turbulence bandwidth increases. The theory fails when m_c and m_1 become comparable so that the internal wave bandwidth becomes small. This will occur at the W-T transition.

Quantification

Dissipation Closure

We now compute the internal wave energy at which the transitions in wavenumber and frequency spectra occur. This requires a relationship between the internal wave energy and the energy dissipation rate ε , which we derive here, and a relationship between the level of the frequency spectrum and that of the wavenumber spectrum, which we derive in the next section.

We use the dissipation rate expression of *Henyey*

et al. [1986], as expanded by *Henyey* [1991], implemented by *Polzin et al.* [1995], and explained by *Winkel* [1998]. The dissipation rate is computed as the net energy fluxing past vertical wavenumber m_c and is written as the product of three terms:

$$\varepsilon = \underbrace{\frac{\phi_{iw} N^2}{2m_c^2} \alpha}_{\text{Energy Density}} \underbrace{\frac{k_H}{m_c} m_c N F r_c^{1/2}}_{\left| \frac{dm}{dt} \right|} \underbrace{\frac{1-r}{1+r}}_{\text{Reflection}}. \quad (10)$$

The first term expresses the energy density at m_c as the product of horizontal kinetic energy and the ratio α of total to horizontal kinetic energy. The second and third terms approximate the net rate at which wave packets cross wavenumber m_c under the influence of vertical shear, S . It uses the ray approximation $\frac{dm}{dt} = -k_H S$, where k_H is the horizontal wavenumber, and a reflection coefficient r , set to 0.4. S is computed from (7). Combining terms, using single wave approximations for α and k_H/m_c , using (8) and referencing to the GM76 spectrum

$$\varepsilon = \varepsilon_0 \frac{m_{cGM}^2}{m_c(m_c - m_1)} \frac{N^2}{N_{GM}^2} \frac{f}{f_{GM}} \Gamma = \varepsilon_0 \frac{m_{cGM}^2}{m_c(m_c - m_1)} \Gamma^* \quad (11)$$

where $\varepsilon_0 = 6.7 \times 10^{-10} \text{ Wkg}^{-1}$ is a reference dissipation rate for the GM spectrum, $m_{cGM} = 0.1 \text{ cpm} = 0.628 \text{ m}^{-1}$ is the value of m_c for the GM spectrum, f_{GM} is evaluated at 27°N and $N_{GM} = 0.00524 \text{ s}^{-1}$. Variations in the energy and wavenumber ratios and the amount of reflection are combined into the Γ factor which equals 1 for a GM spectrum. Similarly, Γ^* absorbs the additional deviations of N and f from GM values. Expression (11) is accurate to about a factor of 2 (*Polzin et al.* [1995], *Winkel* [1998]), if the variations in Γ are included. For completeness, we have not yet assumed $m_1 = 0$.

Substituting for ϕ_{iw} from (8) into (11)

$$\varepsilon = \phi_{iw}^2 \varepsilon_0 \frac{N^2}{N_{GM}^2} \frac{m_{cGM}^2}{F r_c^2} \frac{f}{f_{GM}} \Gamma = \phi_{iw}^2 \varepsilon_0 \frac{m_{cGM}^2}{F r_c^2} \Gamma^*. \quad (12)$$

The dissipation rate is proportional to the internal wave spectral level squared.

Spectral Normalization

The wavenumber and frequency spectra can be predicted as a function of ε using (11), (8) and the forms of $\Phi_{SS}(m)$ (Fig.5) and $\Phi_u^{iw}(\omega)$ (Fig.3). The frequency spectrum is normalized by equating its horizontal kinetic energy in the internal wave band to that in the wavenumber spectrum. The resulting expressions are sensitive to the low mode and low frequency parts of the spectra, which seems unphysical. This, however, is necessary since we do not know the form of the Lagrangian frequency spectra of shear. Integrating (2)

$$\langle U^2 \rangle_L = \int_f^N \Phi_u(\omega) d\omega = \phi_0 f \text{sec}^{-1} \left(\frac{N}{f} \right). \quad (13)$$

Integrating Φ_{SS}/m^2 in Fig.5 while extending the “-1” range to infinity and ignoring the small effect of the B factor in (2), yields

$$\frac{\langle U^2 \rangle_E}{N^2} = \int_{m_1}^{m_b} \frac{\Phi_{uu}(m)}{m^2} dm = \phi_{iw} \left(\frac{1}{m_1} - \frac{1}{2m_c} \right) \quad (14)$$

Solving for ϕ_0 from (13) and (14) with $m_c \gg m_1$ yields

$$\phi_0 = \frac{\phi_{iw} N^2}{m_1 f \text{sec}^{-1}(N/f)}. \quad (15)$$

The W-T Transition Energy

Combining (15), (4), (2), and (11) and assuming $m_1 = 0$ where possible gives

$$\frac{\Phi_w^{turb}(N)}{\Phi_w^{iw}(N)} = \frac{m_1}{m_c} \left[\frac{\pi \beta \varepsilon_0 m_c^2 \Gamma}{2 Fr_c N_{GM}^2 f_{GM}} \right]. \quad (16)$$

The bracketed expression has a value of 0.6, with an uncertainty of at least 50%. The ratios m_1/m_c and $\Phi_w^{turb}(N)/\Phi_w^{iw}(N)$ are nearly equal. The first ratio equals one when the turbulent and internal wave spectra merge in the Lagrangian frequency spectrum. The second equals one when the extrapolated internal wave bandwidth in the Eulerian wavenumber spectrum goes to zero. Both singularities occur at nearly the same internal wave energy, the W-T transition energy. This is the main result of this paper.

Physics

The W-T transition, as computed here, marks the energy level where the basic assumptions of GM-based wave-wave interaction theories fail. At open ocean energy levels and water depths, almost all of the energy is in the internal wave wavenumber band. The transfer of this energy to the smaller scale turbulence is due to wave-wave interactions. *Heney et al.* [1986]’s model of this (12) assumes the interaction of individual “test” waves with the “internal wave” band of wavenumbers in Fig.5. At the W-T transition, m_c and m_1 become nearly equal, this band becomes small and the wave-wave interaction theory becomes ill-posed. In addition, the Richardson number of the lowest wavenumbers, i.e., m_1 , becomes order 1 on average. In places, the Richardson number will be less than critical. The large scale motions are thus locally unstable to shear instability and can thus directly transfer energy to turbulence. This is the physics of stratified turbulence. Thus, the W-T transition marks a change from energy transfer controlled by wave-wave interaction to that controlled by instability and turbulence.

The Transition Energy Level

The energy and spectral level of the W-T transition can be predicted by setting $m_1 = 0$ in (8) and then by finding the internal wave spectral level that sets $m_c = m_1$. This yields

$$\frac{\phi_{trans}}{\phi_{GM}} = \frac{m_c \Gamma}{m_1} \quad (17)$$

where ϕ_{GM} is the value of ϕ_{iw} for the GM spectrum. Note that this is an extrapolation from low energy and thus only tells us when this theory fails.

Similarly, the internal wave energy at the transition is proportional to $N^2 \phi_{iw}/m_1$ by (14), so the wave energy of the transition, relative to GM, is

$$\frac{E_{trans}}{E_{GM}} = \frac{N^2}{N_{GM}^2} \frac{m_c \Gamma}{m_1 \Gamma_{GM}} \quad (18)$$

where m_{1GM} and E_{GM} are the values of m_1 and integrated internal wave energy for the GM spectrum.

Turbulent kinetic dissipation rate is proportional to $N^2 \phi_{iw}^2$ by (12) so

$$\frac{\varepsilon_{trans}}{\varepsilon_0} = \frac{N^2}{N_{GM}^2} \frac{m_{cGM}^2}{m_1^2}. \quad (19)$$

For deep ocean depths ($m_1 = 2\pi/1300\text{m}$, $m_{cGM} = 2\pi/10\text{m}$), the W-T transition is predicted at 130 times the GM spectral level, 130 times the GM energy level and $\varepsilon = 10^{-5}\text{W kg}^{-1}$. This seems unlikely to occur over the entire water column. However, on a continental shelf ($m_1 = 2\pi/100\text{m}$), with $N = N_{GM}$, the W-T transition is predicted at 10 times the GM spectral level, 130 times the GM energy level and $\varepsilon = 7 \times 10^{-8}\text{W kg}^{-1}$. *Moum and Nash [1999]* report values of ε much larger than this over rough topography on the Oregon Shelf. *Gregg et al. [1999]* (this volume) describes significantly larger values on the shelf of Monterey Bay.

Equation (17) predicts that the W-T transition will occur at a lower spectral energy level in shallow water than in deep water. The transition occurs when motions with the same scale as the water depth, i.e. m_1 , have a Richardson number near one. We assume $m_c = 0.1$ cpm, a 10 m wavelength, so in a GM ocean, with m_1 corresponding to a 1300 m wavelength, the internal wave band is a factor of 130 wide. On a 100-meter deep continental shelf, the internal wave band is only a factor of 10 wide, so an increase in internal wave spectral energy level by a factor of 10 above GM will reduce the bandwidth to zero and cause the W-T transition. Note that the same effect does not occur with total internal wave energy density (18) because the total energy is inversely proportional to the water depth (15).

Parameterizations

Quadratic

The change from wave to turbulent physics at the W-T transition implies a change from a quadratic relationship between energy and ε (11) to a linear one (6). In the low energy wave regime, with high Richardson number, dissipation rate is set by wave-wave interactions which are quadratic

in wave energy [*Müller et al., 1986*]. There is ample evidence for this scaling in the ocean thermocline (*Gregg [1989]*, *Polzin et al. [1995]*, *Winkel [1998]*, *Winters and D'Asaro [1997]*). Mixing occurs when the wavefield intermittently decreases the Richardson number below critical, creating turbulence which then restores the Richardson number to above critical. The resulting statistics of Richardson number arrange themselves so that the rate of turbulence generation by instability just matches that set by the wave interactions (*Polzin [1996]*, *Pinkel and Anderson [1997]*). The Richardson number of the large-scale energy containing waves is not important.

Linear

In the high energy, stratified turbulence regime, the dissipation rate is proportional to the energy

$$\varepsilon = C \sigma_w^2 N. \quad (20)$$

Equation (6) implies $C = 0.3 - 0.6$ with the uncertainty set by uncertainty in β . Parameterizations of this form are common in the literature. *Weinstock [1981]* suggests $C = 0.4 - 0.5$ as a good predictor of dissipation in the stratosphere. *Moum [1996]* finds $C = 0.73 \pm 0.06$ for turbulent patches in the ocean thermocline. His measurement of σ_w^2 is biased low by an instrumental high pass filter; this is consistent with an estimate of C which is biased high. Observations in the upper equatorial Pacific, a region of high mean shear and turbulence, show strong linear relationships between turbulent dissipation rate and several measures of internal wave energy (wave isotherm displacement, wave slope, and wave potential energy). (*Moum et al. [1992]*, *Lien et al. [1996]*). We have analyzed the data presented by *Lien et al. [1996]* and find a strong linear relationship ($r^2 = 0.64$) between σ_w^2 , measured from isothermal displacement rate, and ε . The estimated $C = 0.1$, which could easily be biased low by horizontal advection of temperature.

N-scaling of Diffusivity

The diapycnal diffusivity of mass due to internal-wave-driven turbulence is often computed from

$\gamma\varepsilon/N^2$, where the mixing efficiency γ is about 0.2 [Imberger and Ivey, 1991]. For energies below the W-T transition, (11) leads to a diffusivity independent of N and proportional to the internal wave energy squared. For energies above the W-T transition, (6) leads to a diffusivity proportional to $\sigma_w^2 N^{-1}$. Gargett [1984] showed that seasonally averaged diffusivities in lakes and fjords scaled as N^{-1} and proposed this scaling for the ocean interior. Subsequent measurements have showed this to be inappropriate for the ocean. Fjords are usually mixed by vigorous turbulence at a sill (D’Asaro and Lien [1999], Farmer and Freeland [1983]), while lakes are often mixed by the rapid breakdown of intermittent wind-generated seiches [Imberger, 1994]. We suggest that Gargett [1984]’s scaling is appropriate for fjords and lakes because they are mixed by strong turbulence above the W-T transition and inappropriate for the open ocean because it is mixed by motions below the W-T transition.

Summary

Measurements of Lagrangian frequency spectra from neutrally buoyant floats suggest that internal waves are confined to Lagrangian frequencies below N , not surprisingly, and that turbulence is confined to Lagrangian frequencies above N , a stronger statement. Examination of the resulting spectra leads to the hypothesis of two distinct dynamical regimes for mixing in stratified flows. At low energies, flow evolution is controlled by interactions between internal wave modes. At high energies flow evolution is controlled by instabilities of the wave modes. The "Wave-Turbulence" transition, separating these regimes is marked by

- the merging of the internal wave and turbulence spectra at Lagrangian frequency N (Fig.4)
- the decrease of the large scale Richardson number to near one
- the reduction of the internal wave vertical wavenumber bandwidth to a small value (Fig.6)
- A change from a quadratic relationship between wave energy and dissipation rate at low energies (11), to a linear relationship at high energies (6).

Existing parameterizations of the Lagrangian and Eulerian wavenumber spectral shapes (Fig.3,5), combined with the Polzin *et al.* [1995] parameterization of dissipation rate (11), predict that all of the above will occur at the same internal wave energy. The shape of the Lagrangian and Eulerian spectra (Fig.4 and 6) may be useful diagnostics as to whether a given flow is above or below the W-T transition.

The W-T transition is predicted to occur at lower average dissipation rate and internal wave shear, but similar energy density, in shallow water than in deep water (Eq. 17,18,19). It seems unlikely to occur for the full water depth in the open ocean but seems likely to occur at times on the continental shelves. Turbulence parameterization schemes which ignore internal waves will be accurate only for energies above the transition.

References

- Cairns, J., Internal wave measurements from a midwater float, *J. Geophys. Res.*, *80*, 299–306, 1975.
- Cairns, J. L., and G. O. Willaims, Internal wave observations from a midwater float, *2, J. Geophys. Res.*, *81*, 1943–1950, 1976.
- Calman, J., On the interpretation of ocean current spectra. part II: Testing dynamical hypotheses, *J. Phys. Oceanogr.*, *8*, 644–652, 1978.
- Corrsin, S., Estimates of the relations between Eulerian and Lagrangian scales in large Reynold’s number turbulence, *J. Atmos. Sci.*, *20*, 115, 1963.
- D’Asaro, E., Upper ocean temperature structure, inertial currents and Richardson numbers during strong meteorological forcing, *J. Phys. Oceanogr.*, *15*, 943–962, 1985.
- D’Asaro, E. A., and R. C. Lien, Lagrangian measurements of waves and turbulence in stratified flows, *J. Phys. Oceanogr.*, *Submitted*, 1999.

- Dillon, T. M., Vertical overturns: A comparison of Thorpe and Ozmidov length scales, *J. Geophys. Res.*, *87*, 9601–9613, 1982.
- Farmer, D. M., and H. J. Freeland, The physical oceanography of fjords, *Prog. Oceanogr.*, *12*, 147–220, 1983.
- Fofonoff, N. P., Spectral characteristics of internal waves in the ocean, *Deep-Sea Res.*, *16S*, 59–71, 1969.
- Gargett, A. E., Vertical eddy diffusivity in the ocean interior, *J. Mar. Res.*, *42*, 359–393, 1984.
- Gargett, A. E., P. J. Hendricks, T. B. Sanford, T. R. Osborn, and A. J. Williams, III, A composite spectrum of vertical shear in the upper ocean, *J. Phys. Oceanogr.*, *11*, 1258–1271, 1981.
- Garrett, C. J. R., and W. H. Munk, Space-time scales of internal waves: A progress report, *Ann. Rev. Fluid Mech.*, *11*, 339–369, 1975.
- Gregg, M., The study of mixing in the ocean: A brief history, *Oceanography*, *4*, 39–45, 1991.
- Gregg, M., and E. Kunze, Shear and strain in Santa Monica Basin, *J. Geophys. Res.*, *96*, 16,709–16,719, 1991.
- Gregg, M., D. Winkel, and T. Sanford, Varieties of fully resolved spectra of vertical shear, *J. Phys. Oceanogr.*, *23*, 124–141, 1993.
- Gregg, M. C., Scaling turbulent dissipation in the thermocline, *J. Geophys. Res.*, *94*, 9686–9698, 1989.
- Gregg, M. C., D. W. Winkel, J. A. MacKinnon, and R. C. Lien, Mixing over shelves and slopes, in *Internal Wave Modelling, Proceedings, 'Aha Huliko'a Hawaiian Winter Workshop, University of Hawaii at Manoa*, edited by P. Müller, and D. Henderson, p. in press, Hawaii Institute of Geophysics, 1999.
- Heney, F., Why eddy diffusivity doesn't work, in *Internal Gravity Waves and Small-Scale turbulence, Proceedings, 'Aha Huliko'a Hawaiian Winter Workshop, University of Hawaii at Manoa*, edited by P. Müller, and D. Henderson, pp. 245–250, Hawaii Institute of Geophysics, 1989.
- Heney, F., Scaling of internal wave predictions for ε , in *Internal Gravity Waves and Small-Scale turbulence, Proceedings, 'Aha Huliko'a Hawaiian Winter Workshop, University of Hawaii at Manoa*, edited by P. Müller, and D. Henderson, pp. 233–236, Hawaii Institute of Geophysics, 1991.
- Heney, F. S., J. Wright, and S. M. Flatté, Energy and action flow through the internal wave field: An Eikonal approach, *J. Geophys. Res.*, *91*, 8487–8495, 1986.
- Imberger, J., Transport processes in lakes: A review, in *Limnology Now: A Paradigm of Planetary Problems*, edited by R. Margalef, pp. 99–193, Elsevier-Science, New York, 1994.
- Imberger, J., and G. N. Ivey, On the nature of turbulence in a stratified fluid, I. The energetics of mixing, *J. Phys. Oceanogr.*, *21*, 650–658, 1991.
- Kunze, E., M. G. Briscoe, and A. J. W. III, Interpreting shear and strain from a neutrally buoyant float, *J. Geophys. Res.*, *95*, 18,111–18,125, 1990.
- Levine, M., L. Padman, R. D. Muench, and J. H. Morison, Internal waves and tides in the western Weddell sea: Observations from ice station Weddell, *J. Geophys. Res.*, *102*, 1073–1089, 1997.
- Lien, R., M. McPhaden, and M. Gregg, High-frequency internal waves at 0 degrees, 140 degrees w and their possible relationship to deep-cycle turbulence, *J. Phys. Oceanogr.*, *26*, 581–600, 1996.
- Lien, R. C., E. A. D'Asaro, and G. T. Dairiki, Lagrangian frequency spectra of vertical velocity and vorticity in high-Reynolds number oceanic turbulence, *J. Fluid Mech.*, *362*, 177–198, 1998.
- Luyten, P., E. Deleersnijder, J. Ozer, and K. Ruddick, Presentation of a family of turbulence closure models for stratified shallow water flows and preliminary application to the Rhine outflow region, *Cont. Shelf Res.*, *16*, 101–130, 1996.
- Mellor, G. L., and T. Yamada, Development of a turbulence closure model for geophysical fluid problems, *Rev. Geophys. Space Phys.*, *20*, 851–875, 1982.

- Moum, J. N., Energy-containing scales of turbulence in the ocean thermocline, *J. Geophys. Res.*, *101*, 14,095–14,110, 1996.
- Moum, J. N., D. Herbert, C. A. Paulson, and D. R. Caldwell, Turbulence and internal waves at the equator 1. statistics from towed thermistors and a microstructure profiler, *J. Phys. Oceanogr.*, *22*, 1330–1345, 1992.
- Moum, N., and J. Nash, Topographically induced mixing on a small bank on the continental shelf, *Manuscript*, p. 16, 1999.
- Müller, P., D. J. Olbers, and J. Willebrand, The IWEX spectrum, *J. Geophys. Res.*, *83*, 479–500, 1978.
- Müller, P., G. Holloway, F. Henyey, and N. Pomphrey, Nonlinear interactions among internal gravity waves, *Rev. Geophys.*, *24*, 493–536, 1986.
- Munk, W. H., Internal waves and small-scale processes, in *Evolution of Physical Oceanography*, edited by B. A. Warren, and C. Wunsch, pp. 264–291, MIT Press, Cambridge, MA, 1981.
- Pinkel, R., and S. Anderson, Shear, strain and Richardson number variations in the thermocline. part II : Modelling mixing, *J. Phys. Oceanogr.*, *27*, 282–290, 1997.
- Polzin, K., Statistics of the Richardson number: Mixing models and finestructure, *J. Phys. Oceanogr.*, *26*, 1409–1425, 1996.
- Polzin, K., J. Toole, and R. Schmitt, Finescale parameterizations of turbulent dissipation, *J. Phys. Oceanogr.*, *25*, 306–328, 1995.
- Sherman, J., and R. Pinkel, Estimates of the vertical wavenumber-frequency spectrum of vertical shear and strain, *J. Phys. Oceanogr.*, *21*, 292–302, 1991.
- Simpson, J., W.R.Crawford, T. Rippeth, A. Campbell, and J. Cheok, The vertical structure of turbulent dissipation in shelf seas, *J. Phys. Oceanogr.*, *26*, 1579–1590, 1996.
- Sreenivasan, K., On the universality of the Kolmogorov constant, *Phys. Fluids*, *7*, 2788–2784, 1995.
- Weinstock, J., Energy dissipation rates of turbulence in the stable free atmosphere, *J. Atmos. Sci.*, *38*, 880–883, 1981.
- Winkel, D., Influences of mean shear in the Florida current on turbulent production by internal waves, Ph.D. thesis, Univ. of Washington, Seattle, WA 98105, 1998.
- Winters, K. E., and E. A. D’Asaro, Direct simulation of internal wave energy transfer, *J. Phys. Oceanogr.*, *27*, 1937–1945, 1997.
-
- E. A. D’Asaro, Applied Physics Laboratory and School of Oceanography, University of Washington, Seattle, WA
- R. C. Lien, Applied Physics Laboratory, University of Washington, Seattle, WA
-
- This preprint was prepared with AGU’s L^AT_EX macros v4, with the extension package ‘AGU++’ by P. W. Daly, version from .

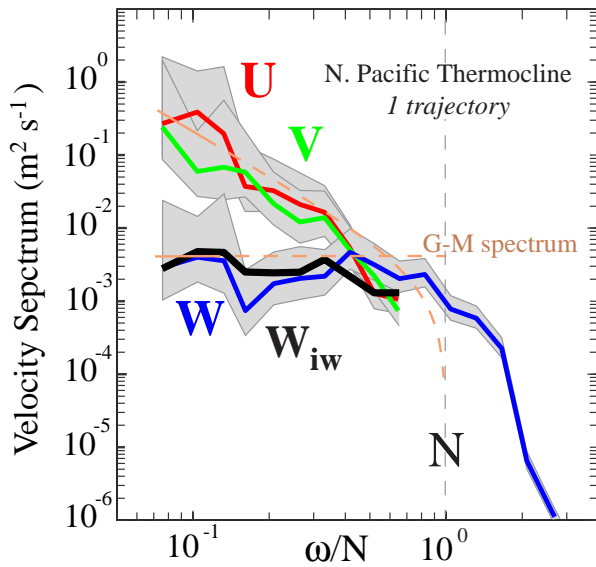


Figure 1. (*D'Asaro and Lien*) Normalized east (red), north (green) and vertical (blue) velocity spectra from the North Pacific thermocline. Shading represents the 95% confidence interval. Black line (W_{iw}) is the vertical velocity spectrum computed from (1). Orange dashed lines are the GM spectrum.

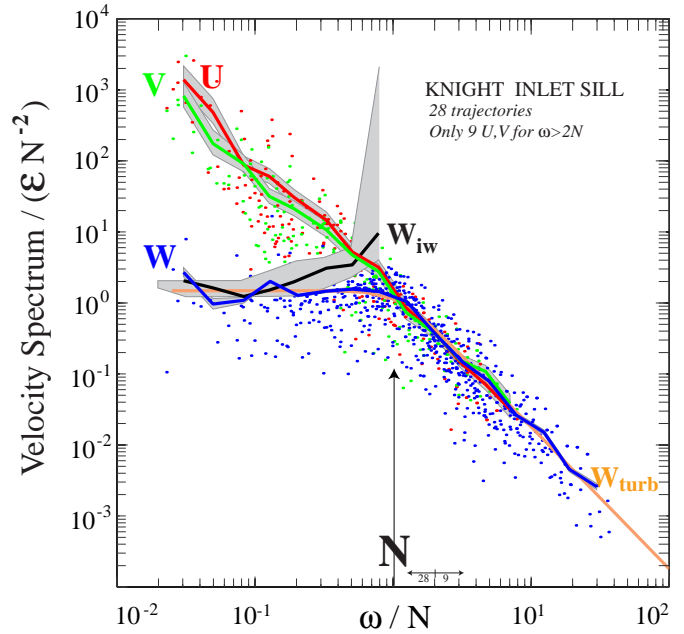


Figure 2. (*D'Asaro and Lien*) Normalized east (red), north (green), and vertical (blue) velocity spectra from the Knight Inlet sill. Dots are individual spectral estimates corrected for instrumental response; lines are average of these; shading represents the 95% confidence interval. Black line (W_{iw}) is the vertical velocity spectrum computed from (1) assuming that horizontal spectra are entirely due to internal waves.